

Two-Dimensional NMR Experiments for Correlating $^{13}\text{C}\beta$ and $^1\text{H}\delta/\epsilon$ Chemical Shifts of Aromatic Residues in ^{13}C -Labeled Proteins via Scalar Couplings

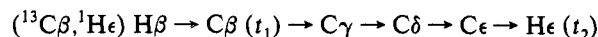
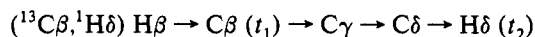
Toshio Yamazaki,^{†,‡} Julie D. Forman-Kay,[†] and Lewis E. Kay^{*,‡}

Division of Biochemistry Research
Hospital for Sick Children, 555 University Avenue
Toronto, Ontario, Canada M5G 1X8
Protein Engineering Network Centres of Excellence and
Departments of Medical Genetics, Biochemistry and
Chemistry, University of Toronto
Toronto, Ontario, Canada, M5S 1A8

Received July 23, 1993

The development of triple-resonance, multidimensional NMR spectroscopy has greatly facilitated the assignment of NMR spectra of ^{15}N , ^{13}C -labeled proteins.^{1–6} This approach is particularly attractive since sequential connectivities are made on the basis of scalar coupling networks and are free of the ambiguities of assignment strategies based on through-space interactions.⁷ The sequence-specific assignment of aromatic ring ^1H and ^{13}C shifts, however, relies on the establishment of NOE connectivities between the $\text{H}\beta$ and $\text{H}\alpha$ protons of the aromatic residue and its associated ring protons. Because of the high density of NOEs involving aromatic protons and the poor dispersion of the aromatic chemical shifts,⁸ it may be difficult to obtain complete assignment of aromatic resonances. Assignment strategies based on deuteration of all but one aromatic amino acid type⁹ can simplify the process but require multiple samples. In this communication we report a simple strategy for the sequence-specific assignment of aromatic residues by providing correlations between the side-chain $^{13}\text{C}\beta$ and ring $^1\text{H}\delta/\epsilon$ chemical shifts. The approach is based exclusively on the transfer of magnetization via scalar couplings.

Figure 1 illustrates the pulse sequences that have been developed to provide $^{13}\text{C}\beta, ^1\text{H}\delta$ and $^{13}\text{C}\beta, ^1\text{H}\epsilon$ correlations. The path of magnetization transfer can be described concisely as follows:



Consistent with the nomenclature for triple resonance experiments, we refer to these experiments as $(\text{H}\beta)\text{C}\beta(\text{C}\gamma\text{C}\delta)\text{H}\delta$ or $(\text{H}\beta)\text{C}\beta(\text{C}\gamma\text{C}\delta\text{C}\epsilon)\text{H}\epsilon$. The basic "building blocks" which have been used to transfer magnetization from the $\text{H}\beta$ to the $\text{H}\delta/\epsilon$ protons have been described in a large number of papers in the literature and will not be reviewed.^{2–6} Instead we focus on a number of important features in the pulse schemes.

Although it is straightforward to implement a 3D version of this experiment by recording $\text{H}\beta$, $\text{C}\beta$, and $\text{H}\delta/\epsilon$ chemical shifts, a 2D version may often be sufficient if resolution in the carbon dimension is maximized. Note that the sensitivity of the 2D version is enhanced by the fact that magnetization from both $^1\text{H}\beta$ protons contributes to a single $^{13}\text{C}\beta, ^1\text{H}\delta/\epsilon$ correlation. Maximum resolution can be achieved, in part, by recording the $^{13}\text{C}\beta$ chemical shift in a constant time manner followed by mirror-image linear prediction¹⁰ after acquisition. The passive $^{13}\text{C}\alpha$ – $^{13}\text{C}\beta$ couplings that would normally be present during the constant time $^{13}\text{C}\beta$ evolution period have been removed by the $90_{\phi 4}$ – ξ – $90_{\phi 4}$ scheme applied at point a in the sequence. The delay ξ is chosen to satisfy the relation $\xi = 1/(2\Delta) - (4/\pi)\tau_{90}$, where Δ is the offset between the centers of the aromatic $^{13}\text{C}\alpha$ and $^{13}\text{C}\beta$ chemical shifts, and τ_{90} is the $90_{\phi 4}$ pulse length. The carrier is positioned in the center of the $^{13}\text{C}\beta$ chemical shift range. Thus, the net result is that the $^{13}\text{C}\beta$ spins are inverted while the $^{13}\text{C}\alpha$ spins are unaffected. Because evolution due to the active $^{13}\text{C}\beta$ – $^{13}\text{C}\gamma$ coupling must proceed during this constant time period, it is important that the $^{13}\text{C}\gamma$ spins not be affected by this scheme. This is readily achieved by adjusting the pulse width, τ_{90} , so that

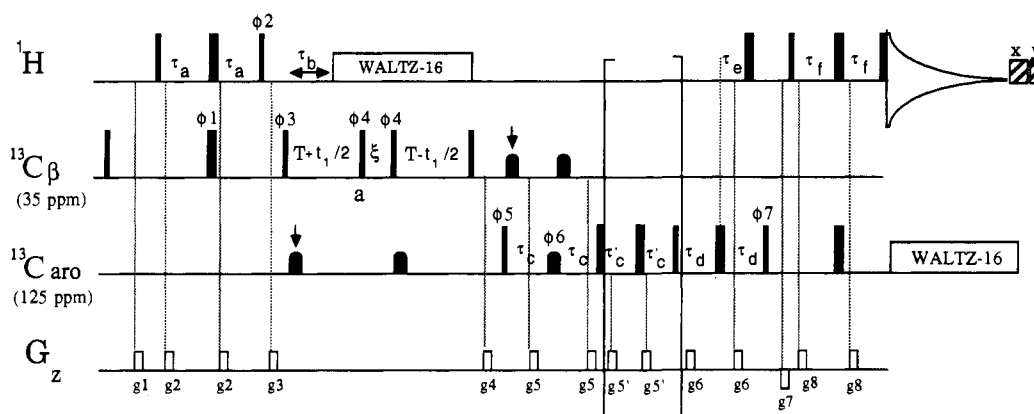


Figure 1. Pulse schemes for the $(\text{H}\beta)\text{C}\beta(\text{C}\gamma\text{C}\delta)\text{H}\delta$ and $(\text{H}\beta)\text{C}\beta(\text{C}\gamma\text{C}\delta\text{C}\epsilon)\text{H}\epsilon$ experiments. The portion of the sequence in parentheses is omitted for the experiment that provides $^{13}\text{C}\beta, ^1\text{H}\delta$ correlations. All narrow (wide) pulses have a flip angle of 90° (180°). Pulses for which the phases are not indicated are applied along the x axis. All carbon pulses are generated using a single synthesizer, with the carbon frequency jumped from 35 to 125 ppm immediately before the pulse of phase $\phi 5$. All carbon 90° pulses, with the exception of the first pulse, for which an 18.5-kHz field is employed, are applied with a 2.9-kHz field, so that application of $^{13}\text{C}\beta$ pulses introduces minimal perturbations of $^{13}\text{C}\gamma$ spins and vice versa.² The shaped $^{13}\text{C}\beta$ and $^{13}\text{C}_{\text{aro}}$ (aromatic) pulses are 180° g_3 pulses¹³ of duration 350 μs and, with the exception of the on-resonance $^{13}\text{C}_{\text{aro}}$ 180° pulse in the middle of the τ_c period, are executed as phase-modulated pulses.^{14,15} All rectangular ^{13}C 180° pulses are at a field of 18.5 kHz. The arrows in the sequence indicate the positions of Bloch–Siegert compensation pulses.¹⁶ ^1H and ^{13}C decoupling are achieved using 4.5- and 3.5-kHz WALTZ-16¹⁷ decoupling fields, respectively. Immediately after acquisition, 10-kHz ^1H purge pulses are applied along the x and y axes for 6 and 3.5 ms, respectively, to aid in the suppression of H_2O . The delays used are $\tau_a = 1.7$ ms, $\tau_b = 1.8$ ms, $\tau_c = 2.7$ ms, $\tau'_c = 3.8$ ms, $\tau_d = 2.1$ ms, $\tau_e = 0.71$ ms, $\tau_f = 1.25$ ms, $T = 4.4$ ms, and $\xi = 71$ μs . The phase cycling employed is $\phi 1 = x$; $\phi 2 = y$; $\phi 3 = x$; $\phi 4 = (x, y, -x, -y)$; $\phi 5 = 4(x), 4(-x)$; $\phi 6 = x$; $\phi 7 = x$; $\text{rec} = x, -x, x, -x, -x, x, -x, x$. Quadrature in t_1 is obtained by States-TPPI of $\phi 3$.¹⁸ The delay, τ'_c , is chosen to maximize the transfer to ^1H . The durations and strengths of the gradients are as follows: $g_1 = (1$ ms, 4 G/cm), $g_2 = (0.5$ ms, 2 G/cm), $g_3 = (1$ ms, 11 G/cm), $g_4 = (2$ ms, 10 G/cm), $g_5 = (1$ ms, 5 G/cm), $g_5' = (0.5$ ms, 5 G/cm), $g_6 = (0.5$ ms, 4 G/cm), $g_7 = (1$ ms, -7 G/cm), $g_8 = (0.5$ ms, 2 G/cm). Delays of at least 50 μs are inserted between the application of a gradient pulse and radio frequency pulses. In the absence of gradients the phase cycle is as follows: $\phi 1 = (x, -x)$; $\phi 2 = (y, -y)$; $\phi 3 = x$; $\phi 4 = 2(x), 2(y), 2(-x), 2(-y)$; $\phi 5 = x$; $\phi 6 = 8(x), 8(y), 8(-x), 8(-y)$; $\phi 7 = 32(x), 32(-x)$; $\text{rec} = 2(2(x, -x, -x, x), 2(-x, x, x, -x)), 2(2(-x, x, x, -x), 2(-x, -x, -x, x))$. A homospoil pulse of 10 ms followed by a recovery delay of 10 ms is inserted in place of g_4 , and the first ^{13}C 90° pulse preceding g_1 is omitted.

$\tau_{90} = \sqrt{15/(4\Delta')}$ where Δ' is the difference, in hertz, between the $^{13}\text{C}\beta$ and $^{13}\text{C}\gamma$ chemical shifts. The removal of the passive $^{13}\text{C}\alpha$ - $^{13}\text{C}\beta$ couplings allows the use of a substantially larger constant time evolution period than would otherwise be possible, resulting in considerable improvements in resolution in the carbon dimension.

Gradients are used in the sequence to suppress artifacts, aid in the removal of water, and minimize the phase cycle employed. The first gradient, g1, is applied after a ^{13}C 90° pulse to eliminate carbon magnetization and to ensure that the observed signal originates on protons.¹¹ The gradient pairs g2, g5, g5', g6, and g8 are applied on opposite sides of refocusing pulses to ensure that only transverse elements are retained.¹² The gradients g3, g4, and g7 are applied when the magnetization of interest is of the form $A_z B_z$. Magnetization not along the z axis, including water magnetization, is effectively dephased by these pulses. Because there is a ^1H 180° pulse following the gradient pair g6 and before g7, the polarity of g7 is inverted relative to g6 to aid in the suppression of water. The final ^1H 90° pulse is inserted to minimize the amount of residual water in the spectra.¹¹

The $(\text{H}\beta)\text{C}\beta(\text{C}\gamma\text{C}\delta)\text{H}\delta$ and $(\text{H}\beta)\text{C}\beta(\text{C}\gamma\text{C}\delta\text{C}\epsilon)\text{H}\epsilon$ experiments were recorded on a 1.5 mM sample of a recombinant C-terminal SH2 domain of PLC- γ_1 (105 amino acids) complexed with a 12-residue phosphopeptide from the platelet-derived growth factor receptor (PDGFR), in 90%/10% $\text{H}_2\text{O}/\text{D}_2\text{O}$, 0.1 M Na phosphate, pH 6.2, 30 °C. The experiments were performed on a Varian UNITY 500-MHz spectrometer equipped with a pulsed field gradient unit and a triple resonance probe with an actively shielded z gradient. Figure 2 shows the data obtained: 12 of the 15 $^{13}\text{C}\beta$, $^1\text{H}\delta$ correlations are present, while six of the nine $^{13}\text{C}\beta$, $^1\text{H}\epsilon$ cross peaks are present. Certain correlations involving F74, Y83, and Y84, residues implicated in peptide binding, are missing, confirming previous results demonstrating a broadening of aliphatic resonances from residues lining the binding site. The peak marked with an X in Figure 2 is due to conformational heterogeneity of H23; a multiplicity of peaks associated with this residue has been observed in other experiments. While not observed in the present study, strong coupling between aromatic carbons may give rise to weak $^{13}\text{C}\beta$, $^1\text{H}\epsilon$ cross peaks in the $(\text{H}\beta)\text{C}\beta(\text{C}\gamma\text{C}\delta)\text{H}\delta$ experiment.

In this communication we have presented an experiment for correlating $^{13}\text{C}\beta$ and $^1\text{H}\delta/\epsilon$ chemical shifts of aromatic residues based on scalar connectivities. Although pulsed field gradients have been employed in the present experiment, their use is not essential. The experiment can be performed on either H_2O or D_2O samples with good sensitivity and provides a simple approach for the unambiguous sequence-specific assignment of aromatic side chains.

Acknowledgment. Valuable discussions with Dr. Lawrence McIntosh, University of British Columbia, are acknowledged. Toshio Yamazaki is the recipient of a Human Frontiers Science Program Fellowship. The authors are grateful to Mr. Alex Singer for preparation of the SH2 sample used in the present study and Dr. S. Shoelson, Harvard University, for the gift of pY1021 phosphopeptide.

[†] Hospital for Sick Children.

[‡] University of Toronto.

(1) Ikura, M.; Kay, L. E.; Bax, A. *Biochemistry*, **1990**, *29*, 4569.

(2) Kay, L. E.; Ikura, M.; Tschudin, R.; Bax, A. *J. Magn. Reson.* **1990**, *89*, 496.

(3) Clubb, R. T.; Thanabal, V.; Wagner, G. *J. Biomol. NMR* **1992**, *2*, 203.

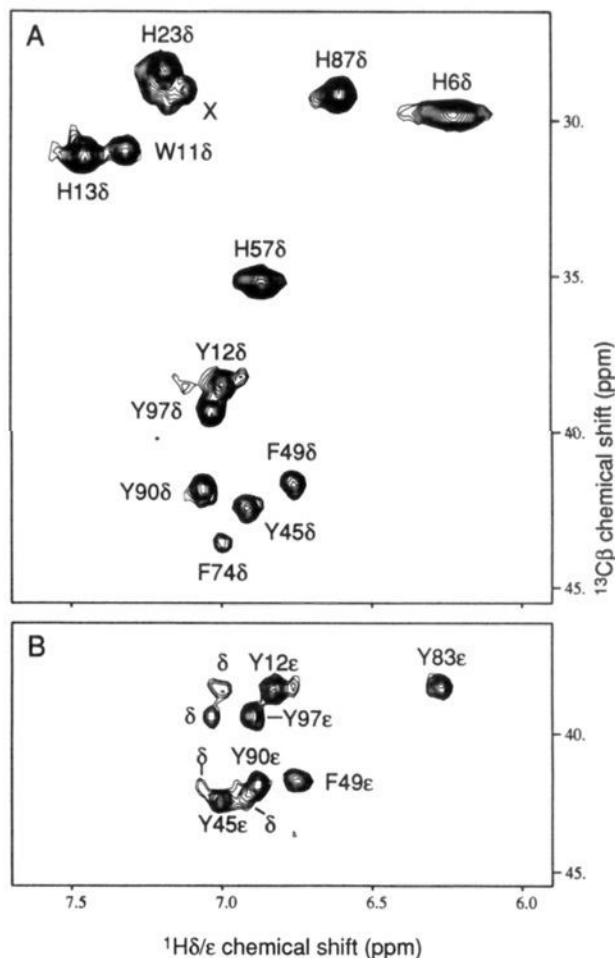


Figure 2. 2D spectra showing the $^{13}\text{C}\beta$, $^1\text{H}\delta$ correlation map (A) and a portion of the $^{13}\text{C}\beta$, $^1\text{H}\epsilon$ correlation map (B) for the C-terminal SH2 domain of PLC- γ_1 complexed with an unlabeled 12-residue phosphotyrosine peptide from PDGFR. Both data sets were recorded with acquisition times of 8 ms in t_1 , 1024 scans per complex t_1 point, and relaxation delays of 0.9 s to give measuring times of ~ 20 h/spectrum. Mirror-image linear prediction¹⁰ was employed in the t_1 time domain to improve the resolution.

(4) Grzesiek, S.; Bax, A. *J. Am. Chem. Soc.* **1992**, *114*, 6291.

(5) Farmer, B. T.; Venters, R. A.; Spicer, L. D.; Wittekind, M. G.; Muller, L. *J. Biomol. NMR* **1992**, *2*, 195.

(6) Palmer, A. G.; Fairbrother, W. J.; Cavanaugh, J.; Wright, P. E.; Rance, M. *J. Biomol. NMR* **1992**, *2*, 103.

(7) Wuthrich, K. *NMR of Proteins and Nucleic Acids*; Wiley: New York, 1986.

(8) Yamazaki, T.; Yoshida, M.; Nagayama, K. *Biochemistry* **1993**, *32*, 5656.

(9) McIntosh, L. P.; Wand, A. J.; Lowry, D. R.; Redfield, A. G.; Dahlquist, F. W. *Biochemistry* **1990**, *29*, 6341.

(10) Zhu, G.; Bax, A. *J. Magn. Reson.* **1990**, *90*, 405.

(11) Kay, L. *J. Am. Chem. Soc.* **1993**, *115*, 2055.

(12) Bax, A.; Pochapsky, S. *J. Magn. Reson.* **1992**, *99*, 638.

(13) Emsley, L.; Bodenhausen, G. *Chem. Phys. Lett.* **1987**, *165*, 469.

(14) Boyd, J.; Scoffe, N. *J. Magn. Reson.* **1989**, *85*, 406.

(15) Patt, S. L. *J. Magn. Reson.* **1992**, *96*, 94.

(16) Vuister, G. W.; Bax, A. *J. Magn. Reson.* **1992**, *98*, 428.

(17) Shaka, A. J.; Keeler, J.; Frenkiel, T.; Freeman, R. *J. Magn. Reson.* **1983**, *52*, 335.

(18) Marion, D.; Ikura, M.; Tschudin, R.; Bax, A. *J. Magn. Reson.* **1989**, *85*, 393.